PVA/pectin/ZnO nanocomposites as antibacterial compounds for root canal treatment

Mohsen Safaei[1), 2)] (ORCID ID: 0000-0003-3885-6640), **Ramin Ahmadi**[3)] (0009-0002-7046-2633), **Mohammad Salmani Mobarakeh**[2)] (0000-0002-3272-4041), **Roohollah Sharifi**[2), 4)] (0000-0001-7917-5409), **Ling Shing Wong**[5)] (0000-0002-5869-0804), **Shraddha Rathi**[6)] (0000-0001-5657-0692), **Amina**[6)] (0000-0002-7518-9050), **Shaista Afroz**[6), *)] (0000-0003-1941-8725)

DOI: https://doi.org/10.14314/polimery.2025.5.4

Abstract: Structure and antibacterial activity of PVA/pectin/ZnO nanocomposites were investigated. The Taguchi method was used to select the optimal composition of the composites, considering the effect of PVA, pectin and ZnO on the biocidal properties. Various methods were used to characterize composites, including FT-IR, XRD, FESEM, EDS, TEM, elemental mapping, and TGA. The strong antibacterial properties of PVA/pectin/ZnO and complete inhibition of *Enterococcus faecalis* biofilm development were confirmed. The developed nanocomposites can be used in various fields as antimicrobial agents.

Keywords: PVA, pectin, ZnO nanoparticles, human health, nanocomposites.

Nanokompozyty PVA/pektyna/ZnO jako związki antybakteryjne do leczenia kanałowego

Streszczenie: Zbadano strukturę i aktywność przeciwbakteryjną nanokompozytów PVA/pektyna/ZnO. Do wytypowania optymalnego składu kompozytów stosowano metodę Taguchi, uwzględniającą wpływ PVA, pektyny i ZnO na właściwości biobójcze. Do charakterystyki kompozytów stosowano różne metody, w tym FT-IR, XRD, FESEM, EDS, TEM, mapowanie pierwiastków i TGA. Potwierdzono silne właściwości przeciwbakteryjne PVA/pektyna/ZnO i całkowite zahamowanie rozwoju biofilmu *Enterococcus faecalis*. Opracowane nanokompozyty mogą być stosowane w różnych dziedzinach jako środki przeciwdrobnoustrojowe.

Słowa kluczowe: alkohol poliwinylowy, pektyna, nanocząsteczki ZnO, zdrowie człowieka, nanokompozyty.

The oral cavity is one of the most favorable environments of the human body for the growth of pathogens and bacterial biofilms, which includes several surfaces such as the hard tissue of the teeth, dental plaques, and the tongue, and each of them creates special conditions for the growth of different bacterial species. Biofilms are polymicrobial, creating a dynamic microenvironment where interactions between the different layers are complex due to presence of diverse bacterial composition. This complexity of biofilm makes it challenging to treat it with antibiotics [1, 2]. One of the major causes of root canal treatment failure is the presence of residual bacteria; among these bacteria, *Enterococcus faecalis* (*E. faecalis*) is the most seen. Opportunistic pathogens include the gram-positive facultative anaerobic bacterium E. *faecalis*. E. *faecalis* can form a biofilm alone without the support of other bacteria, and due to its various mechanisms and metabolic pathways, it can survive in unfavorable environments [3]. Although a significant number of studies have focused on the synthesis of new antimicrobial agents to overcome this problem, most of these efforts could not achieve the desired results due to the rapid degradation and release of antibacterial agents [4, 5]. According to the existing problems, a new method of controlling biofilms is needed to overcome this challenge of the new era. With the advancement of nanoscience, nanomaterials are considered as the

---

[1)] Division of Dental Biomaterials, School of Dentistry, Kermanshah University of Medical Sciences, Kermanshah 54658, Iran.

[2)] Advanced Dental Sciences and Technology Research Center, School of Dentistry, Kermanshah University of Medical Sciences, Kermanshah 38647, Iran.

[3)] Students Research Committee, Kermanshah University of Medical Sciences, Kermanshah 54658, Iran.

[4)] Department of Endodontics, School of Dentistry, Kermanshah University of Medical Sciences, Kermanshah 54658, Iran.

[5)] Faculty of Health and Life Sciences, INTI International University, Nilai 71800, Malaysia.

[6)] Department of Prosthodontics, ZA Dental College, Aligarh Muslim University, Aligarh, Utar Paradesh 202002, India.

[*)] Author for correspondence: shaista_afroz@yahoo.com

antimicrobial agent with a promising future application. Nanoparticles can easily prevent the formation of biofilms and bacterial growth by mechanisms that antibiotic resistance genes and structural features of biofilms are not programmed to deal with [6, 7]. Nanoparticles have high surface energy and a big surface area, which causes them to climb together. A decrease in reactive oxygen species (ROS) occurs because of this. Hence, a polymer matrix capable of efficiently guiding nanoparticles is necessary [8]. Zinc oxide (ZnO), magnesium oxide (MgO), titanium dioxide (TiO_2), silicon dioxide (SiO_2), calcium oxide (CaO), and several inorganic metal oxides have been found to possess antibacterial capabilities, including biocidal and bacteriostatic actions [9-11]. It is necessary to examine TiO_2, MgO, CaO, and ZnO with more precision because these materials are not only stable under extreme circumstances, but they are also known to be harmless to humans [12, 13].

Nanoparticles of ZnO are one of the most popular and efficient antimicrobial substances. ZnO nanoparticles have been found to be more efficient against *E. faecalis* and other Gram-positive bacteria than against Gram-negative bacteria, according to research [14, 15]. ZnO has several uses due to its unusual physical and chemical characteristics, such as its highlight stability, broad spectrum of radiation absorption, and strong electrochemical coupling coefficient. The pharmaceutical and food packaging sectors are two of the several that make use of ZnO [16]. People are hoping for a lot because of how cheap it is to make compared to other chemicals [17].

Past research has demonstrated that ZnO has antibacterial properties against numerous Gram-positive and Gram-negative bacteria, including *Staphylococcus aureus*, *E. faecalis*, *Salmonella typhimurium*, and *Enterobacter pathogens* [18]. ZnO nanoparticles near the external surface of the bacteria cause ROS production, which causes damage to the bacterial cell wall and causes the leakage of RNA, proteins, and K^+ from the bacterial cell and finally the death of the bacteria [17].

Polyvinyl alcohol (PVA) is a synthetic hydrophilic linear polymer that has many uses in medical and pharmaceutical fields with its special chemical and physical properties [19]. Studies have shown that the use of PVA is safe even at high levels of consumption. Also, this substance is a suitable option for drugs that require long-term use in the stable release of nanoparticles [20].

The efficiency of the synthesized nanocomposite can be increased by adding an agent to create a controlled release of the drug, Pectin, a plant linear polysaccharide, is such a successful choice of an agent at whose addition to nanocomposite leads to a controlled drug release [21]. Pectin adds many other useful properties to the nanocomposite, including increasing drug loading efficiency, reducing early drug release, and controlling drug release behavior according to the type of drug and target tissue [22]. To overcome the limitations of thermal stability and mechanical properties, pectin is combined with PVA to form a nanocomposite matrix [23].

The aim of this study was to determine the optimal conditions for the synthesis of a nanocomposite with maximum antibacterial activity against *Enterococcus faecalis* biofilm. To the best of our knowledge, nanocomposites of PVA, pectin, and ZnO have been obtained for the first time.

EXPERIMENTAL PART

Materials

Zinc acetate dihydrate (Merck, Germany), sodium hydroxide (Aldrich, USA), PVA (Merck, Germany), pectin (Sigma Aldrich, USA), potassium bromide (Merck, Germany), brain heart infusion (BHI, Quelab, Canada), brain heart infusion agar (BHIA, Merck, Germany) were used in this study.

ZnO nanoparticles synthesis

To synthesize ZnO nanoparticles, zinc acetate and sodium hydroxide (NaOH) were dissolved in deionized water to obtain a solution with a concentration of 0.1 M and 0.2 M, respectively. Thereafter, the two solutions were combined in a beaker and kept the temperature at 60°C for 2 h while stirring at 750 rpm. A clear, milky solution was first generated after 120 min. After that, a white product was precipitated by centrifuging the solution at 5,000 rpm for 120 s. A combination of distilled water and acetone was used to wash the precipitated product. By subjecting the mixture to an oven drying cycle at 75°C for a duration of 6 h, powdered ZnO nanoparticles were produced [24].

PVA/pectin/ZnO composites preparation

Based on the Taguchi method, the composition of the composites was selected (Table 1). PVA, pectin and ZnO in appropriate proportions were pre-mixed for 60 min using a magnetic stirrer and then mixed for 20 min at 40°C using an ultrasonic homogenizer. The obtained composites were dried in an oven at 80°C for 24 h [24].

Table 1. Taguchi data for the analysis of experiments related to the preparation of PVA/pectin/ZnO composites

Sample	PVA mg/mL	Pectin mg/mL	ZnO mg/mL
1	1.5	5	2
2	1.5	7.5	4
3	1.5	10	6
4	3	5	4
5	3	7.5	6
6	3	10	2
7	4.5	5	6
8	4.5	7.5	2
9	4.5	10	4

Methods

FT-IR

Chemical structure was conducted by Fourier transform infrared spectroscopy (FT-IR) using ThermoFisher Scientific spectrometer (Waltham, USA). The spectra were recorded using at least 32 scans with 2 cm^{-1} resolution, in the spectral range of 4000-400 cm^{-1}, using KBr pellets technique.

XRD

Crystal structure was determined by X-ray diffraction spectroscopy (XRD) using Philips X' Pert (Amsterdam, the Netherlands) diffractometer with monochromatic CuK α radiation (γ = 0.154056 nm) at 40 kV and 30 mA, and 2θ angles of 20-80°.

FESEM

A high-resolution field emission scanning electron microscope (FESEM), model MIRA3 (TESCAN, Brno, Czech Republic), at a voltage of 30 kV was used for structure analysis.

EDS

Elements distribution maps were determined by employing X-ray energy diffraction spectroscopy (EDS) with Bruker (Billerica, MA, USA) type equipment. A high-resolution scanning electron microscope equipped with a SAMX X-ray energy detector was used to conduct this study.

TEM

A transmission electron microscope (TEM), model EM208S from Philips (Amsterdam, The Netherlands), was used to study the morphology of the nanocomposites at a voltage of 100 kV and in the range of 200–800 nm.

Thermogravimetric analysis

Thermogravimetric analysis (TGA) using TA Q600 (New Castle, DE, USA) was used to study thermal properties. The measurements were performed in an argon atmosphere, at a heating rate of 20°C/min and in the temperature range of 25–800°C.

Antibacterial activity

The antibacterial efficacy of obtained nanocomposites against *E. faecalis* was investigated using the colony forming unit (CFU) technique. Brain heart infusion (BHI) medium was used to culture *E. faecalis*, which was received from Iran's National Center for Genetic and Biological Resources. After 24 hours of incubation in BHI culture medium, the bacteria were transferred to a 0.5 McFarland solution to create a microbial suspension with 1.5×10^8 CFU/ml. By combining 1 mL of culture media with 100 μL of *E. faecalis* bacterium, nine independent experiments were conducted to determine the effects of various nanocomposites concentrations. Once the incubation period was over, 100 μL of suspension with varying concentrations was incubated in BHI agar medium. At last, after incubation for 24 h, the quantity of colonies was recorded [25]. Qulitek-4 software was used to calculate and identify the ideal circumstances for the preparation of nanocomposites with the highest antibacterial activity.

RESULTS AND DISCUSSION

Antibacterial activity

Figure 1 displays the antibacterial activity of nanocomposites obtained using the Taguchi method against the *E. faecalis* bacteria. Sample 5 shows the highest antibacterial effect (0 $\log_{10}$ CFU/mL). On the other hand, sample 1 exhibits the weakest antibacterial activity, measuring 2.37 $\log_{10}$ CFU/mL. Consistent with earlier research on the components' antibacterial capabilities, these findings were significant [24]. Figure 2 shows the antibacterial action of PVA/pectin/ZnO nanocomposites as a function of the levels of the examined variables. According to the results, the effectiveness of suppressing the growth of *Enterococcus faecalis* was best achieved by using three levels of nanoparticles including PVA, pectin, and ZnO. Level 3 of all examined variables demonstrated survival rates for these bacteria of 0.48, 0.77, and 0.34 $\log_{10}$ CFU/mL, respectively. The interplay between the investigated variables and the *Enterococcus faecalis* survival rate is detailed in Figure 3. In terms of reducing bacterial growth, the interaction between the second and third levels of pectin and ZnO was the most significant (55.90%). At contrast, the interaction between PVA and pectin was found to be the weakest (1.26%) at the second level. PVA (44.61%) and ZnO nanoparticles (35.22%) were the most effective components in suppressing *Enterococcus faecalis* growth,

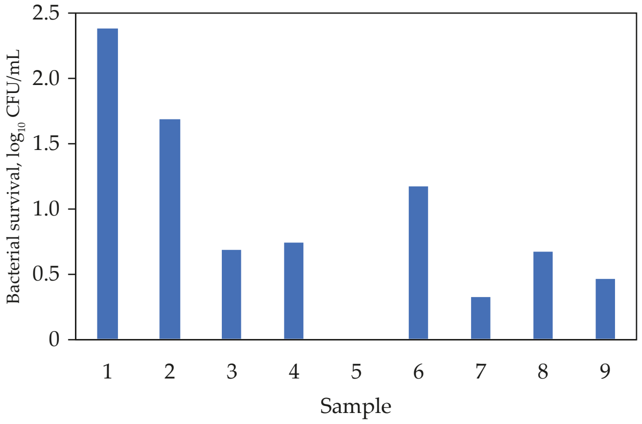

Fig. 1. Survival rate of *Enterococcus faecalis* of composites

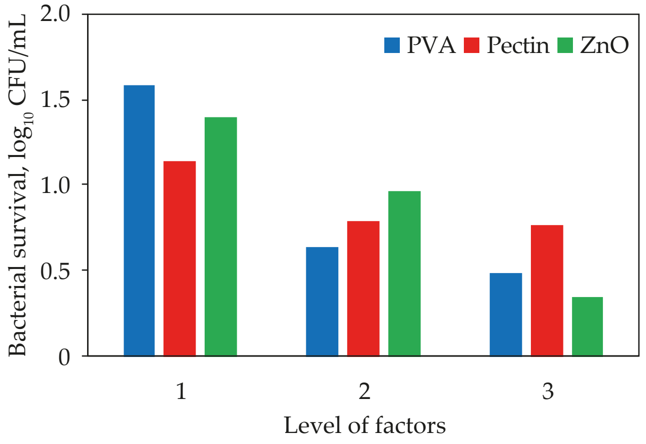

Fig. 2. Effect of different levels of PVA, pectin and ZnO on the survival rate of *E. faecalis*.

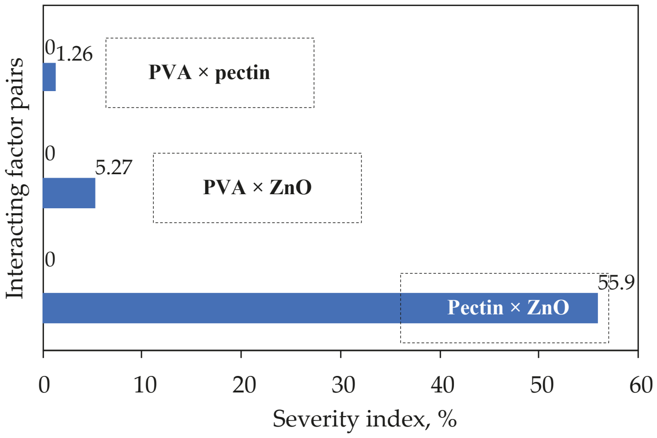

Fig. 3. Effect of factors studied on the survival rate of *E. faecalis*.

Table 2. Factors influencing the limitation of *Enterococcus faecalis* survival

Factors	DOF*	Sum of squares	Variance	F-Ratio, F	Pure sum	Percent
PVA	2	2.13	1.06	10.52	1.93	44.61
Pectin	2	0.26	0.13	1.31	0.06	1.43
ZnO	2	1.72	0.86	8.52	1.52	35.22

*) DOF - degree of freedom

according to the analysis of variance. It is clear from Table 2 that pectin has the least effect on bacterial survival (1.43%). The third level was shown to be the most appropriate for pectin, ZnO, and PVA (Table 3). Under these circumstances, the nanocomposite should be able to inhibit bacterial growth to a level as low as 0.21 $\log_{10}$ CFU/mL.

Table 3. Optimal conditions for the synthesis of PVA/Pectin/ZnO nanocomposite with the highest antibacterial activity

Factors	Level	Contribution
PVA	3	0.42
Pectin	3	0.13
ZnO	3	0.56
Total contribution from all factors		1.11
Current grand average of performance		0.90
Bacterial survival at optimum condition		-0.21

Structure analysis

Figure 4 shows the UV-Vis spectra of PVA, pectin, ZnO and PVA/pectin/ZnO nanocomposite. The spectrum of PVA shows a peak at 214 nm [26]. In the case of pectin, a specific absorption peak is observed at 284 nm. Several parameters such as energy band, oxygen deficiency, surface roughness and impurity centers determine the absorption rate of the sample containing ZnO nanoparticles. An absorption peak at around 370 nm is observed in the spectrum of ZnO [27]. In the spectrum of PVA/pectin/ZnO, two absorption peaks at 220 and 368 nm are detected, corresponding to PVA and ZnO, respectively.

Figure 5 shows FT-IR spectra, which confirms the interactions between the nanocomposite components. In FT-IR spectrum of PVA, there is an intense peak at wave number 3424 cm^{-1} originating from O-H bonds, and at wave numbers 2955 cm^{-1} and 2925 cm^{-1}, there are bands from C-H stretching vibrations. The peak at 1650 cm^{-1} is also related to the stretching vibrations of C=O bonds. Moreover, in PVA, the peak at 1420 cm^{-1} corresponds to the stretching vibrations of the O-H group, and the peak at 1291 cm^{-1} was the stretching vibration of the C-O group [28]. In the FT-IR spectrum of pectin, the bands in the range from 2500 to 3400 cm^{-1} indicate the presence of hydroxyl groups (O-H).

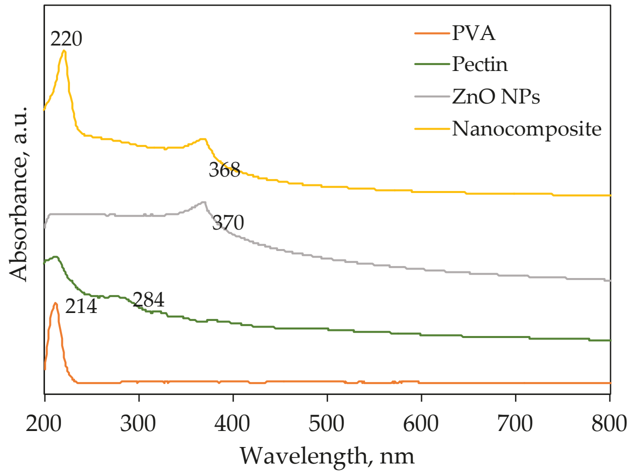

Fig. 4. UV-VIS spectra of PVA, pectin, ZnO and PVA/pectin/ZnO nanocomposite

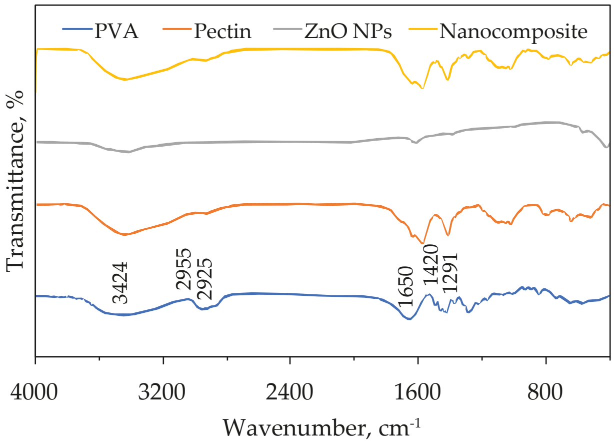

Fig. 5. FT-IR spectra of PVA, pectin, ZnO NPs and nanocomposite

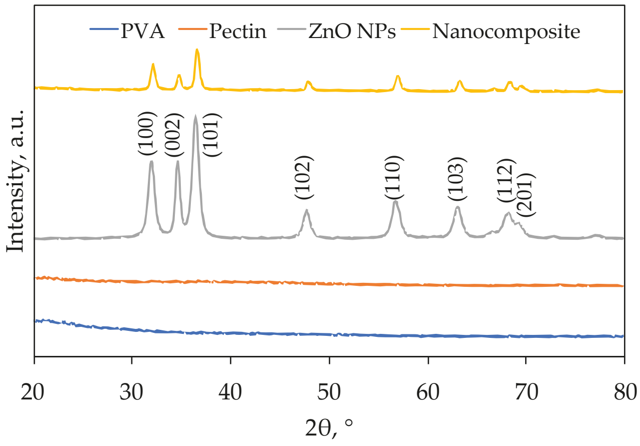

Fig. 6. XRD patterns of PVA, pectin, ZnO NPs and the nanocomposite

The bands in the range of 1400--1650 cm^{-1} are attributed to the C=O stretching vibrations, and the bands in the range from 950 to 1200 cm^{-1} to the C-O stretching vibrations [29]. The broad absorption band in the frequency of 3000-3660 cm^{-1} observed in the FT-IR spectrum of ZnO nanoparticles is attributed to the flexibility of the O-H group caused by the residual alcohols, water, and Zn-OH. Moreover, in the spectrum of ZnO at the wave number of 1635 cm^{-1} there is a band corresponding to the bending vibrations of the H-OH bond. The broadest and strongest absorption bands occur at 435 cm^{-1} and 560 cm^{-1}, originating from the stretching vibrations of Zn-O [30]. FT-IR results confirmed the structure of PVA/pectin/ZnO nanocomposite.

X-ray diffraction analysis was used to examine the phase characteristics and crystalline behavior of the nanocomposite and its components (Figure 6). A wide peak near 2θ of 20° and another peak at 22° are visible in the X-ray pattern of PVA, suggesting a crystal reflection. The presence of both crystalline and amorphous phases in PVA's semi-crystalline structure is confirmed by these two broad peaks, which are distinctive of the compound and reflect the (101) and (101) planes, respectively [31]. The presence of a pure pectin phase and its complicated structure are shown by the X-ray diffraction pattern of pectin, which is at 2θ equal to 26.5 degrees. The amorphous structure of pure pectin [32] is responsible for the three large peaks observed at 2θ = 14°, 20°, and 30°. ZnO nanoparticles XRD pattern revealed a hexagonal crystal structure in the zincite phase. The plates (hkl), (002), (101), (102), (110), (103), (112) and (201) had calculated Miller indices at 2θ, 32.06 and 71.0 angles, with corresponding values of 34, 36.51, 47.90, 56.95, 63.26, 68.20 and 69.30. Peaks intensity in the nanocomposite spectrum decreased compared to the XRD patterns of the original materials. The interaction between the polymer matrix materials and the ceramic nanoparticles changes the spacing between the plates, which indicates the formation of the nanocomposite.

Figure 7 shows the structure of pectin macromolecule (Fig. 7a), ZnO nanoparticles (Fig. 7b) and PVA/pectin/ZnO nanocomposite (Fig. 7c). Due to their small size and high surface to volume ratio, ZnO nanoparticles aggregate and agglomerate in the PVA matrix.

TEM images of the nanocomposite (Figure 8) were taken at different magnifications, which allowed to observe the size, shape, and arrangement of the composite components. Darker spots in TEM image represent areas of higher density surrounded by lower density polymer matrix. This phenomenon allows to gain insight into the

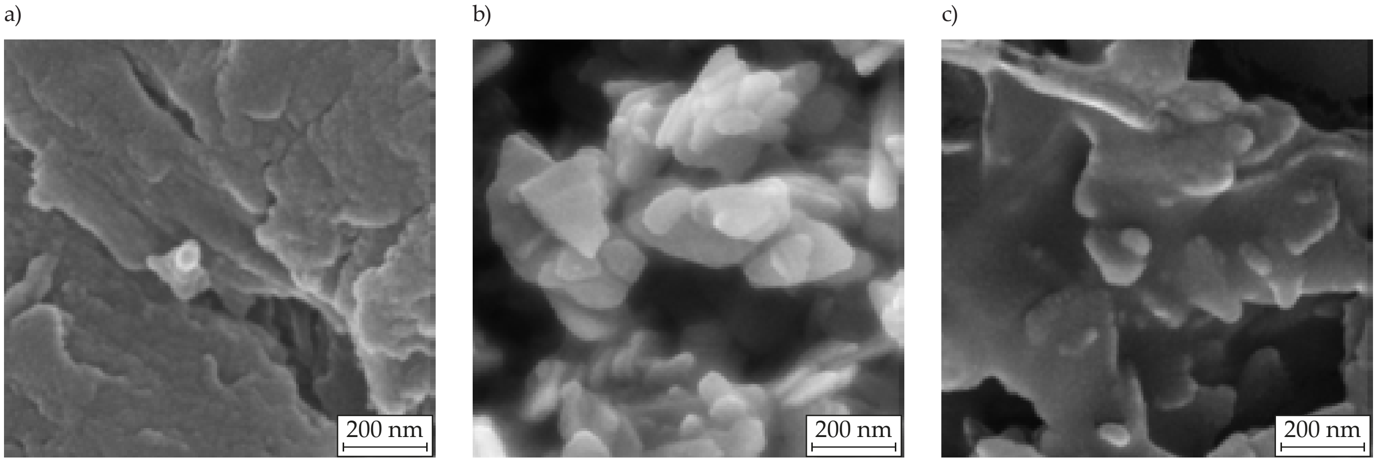
a) b) c)

Fig. 7. SEM images: a) pectin, b) ZnO NPs, c) PVA/pectin/ZnO nanocomposite

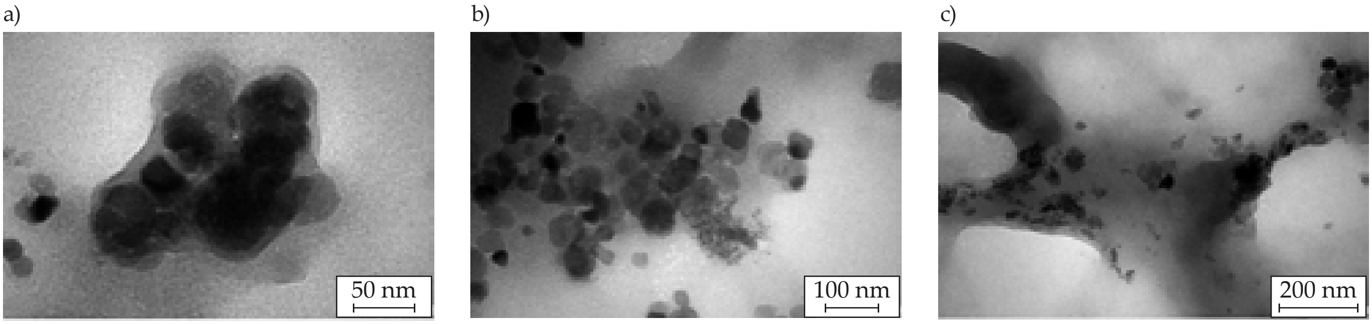

Fig. 8. TEM images of PVA/pectin/ZnO nanocomposite

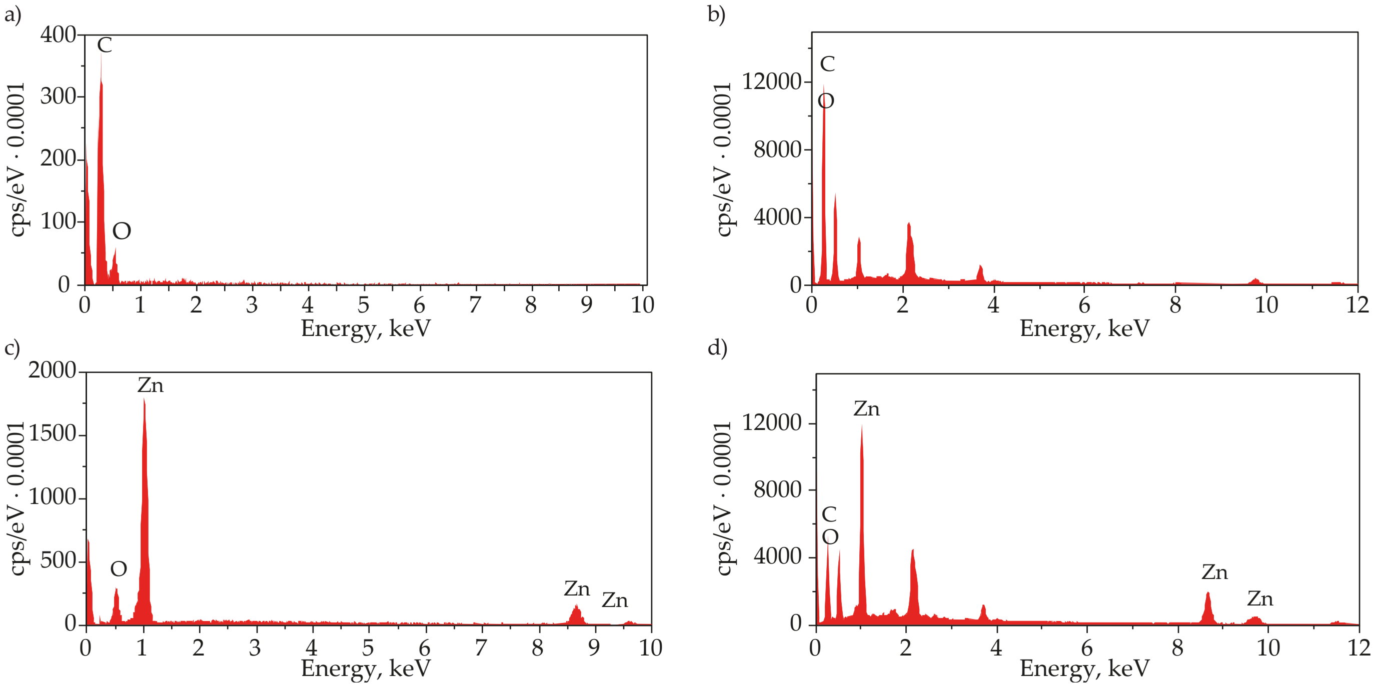

Fig. 9. EDS patterns: a) PVA, b) pectin, c) ZnO NPs, d) PVA/pectin/ZnO nanocomposite

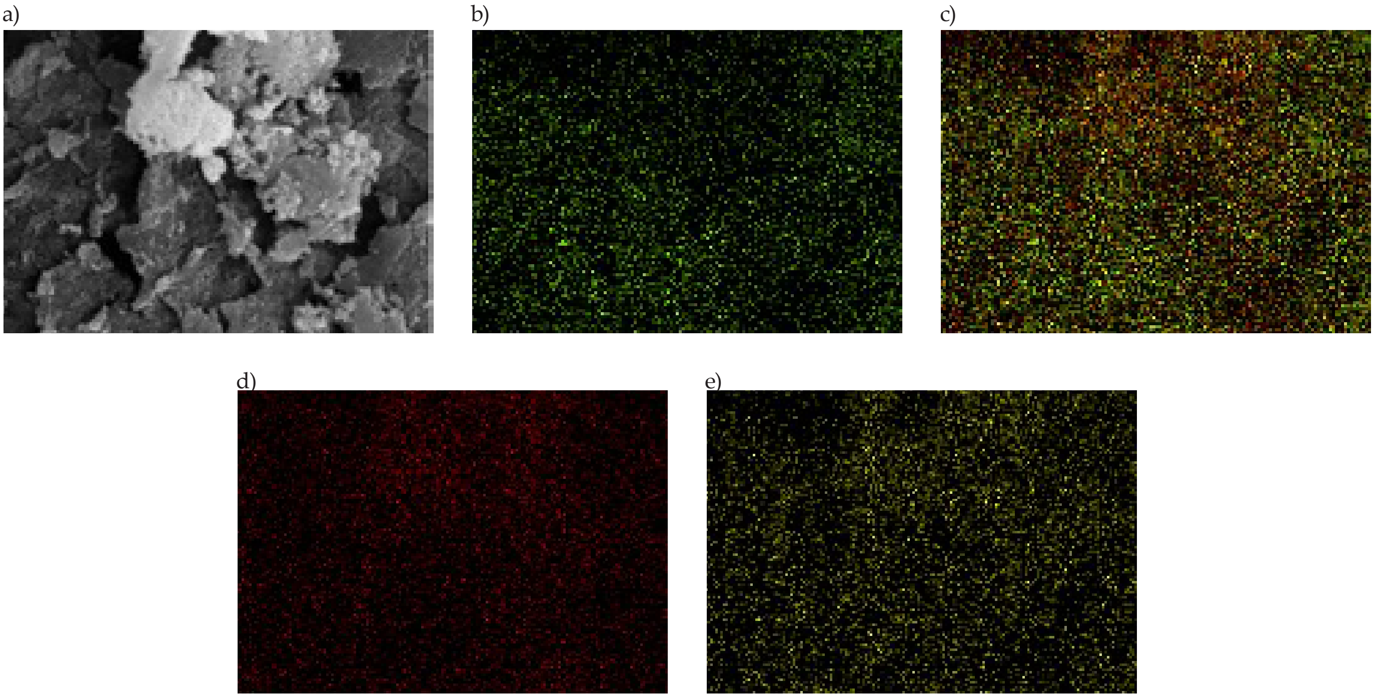

Fig. 10. Dispersion map: a) PVA/pectin/ZnO nanocomposite, b) all elements, c) carbon, d) zinc, e) oxygen

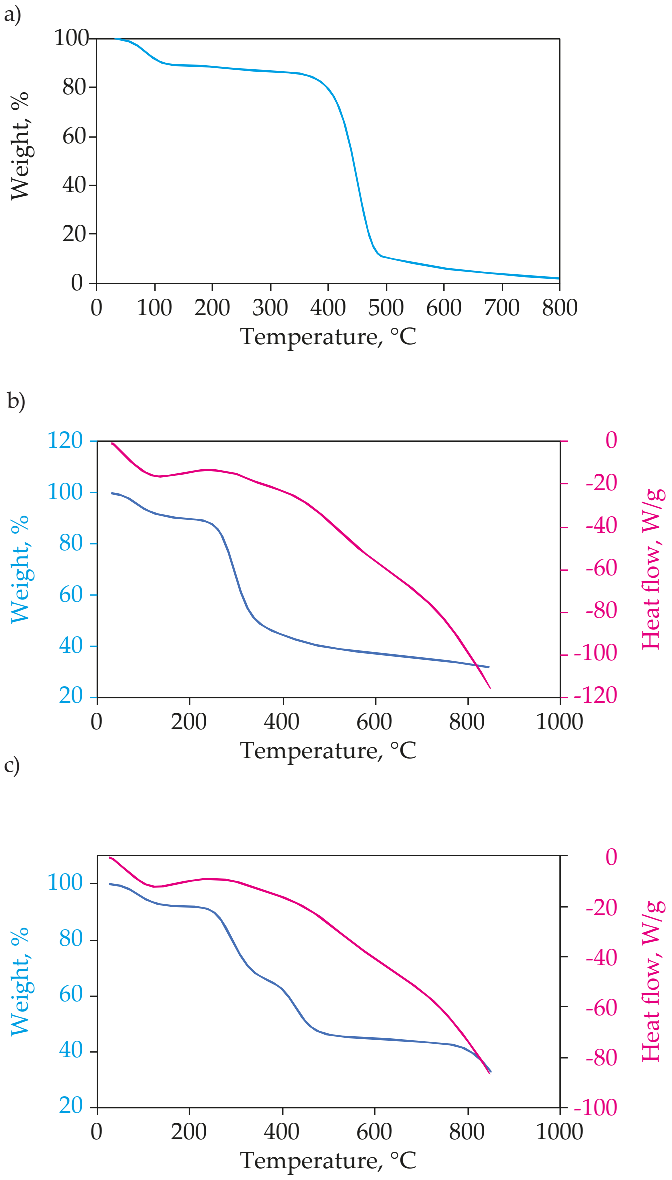

Fig. 11. Thermogravimetric curves: a) PVA, b) pectin, c) PVA/pectin/ZnO nanocomposite

composition of the nanocomposite components as well as into the formation of the composite structure [33].

X-ray energy diffraction (EDS) analysis showed that PVA contains 71.9 wt% carbon and 28.03 wt% oxygen (Fig. 9a), pectin contains 44.51 wt% carbon and 55.49 wt% oxygen (Fig. 9b), and ZnO contains 64.11 wt% zinc and 35.69 wt% oxygen (Fig. 9c). While the nanocomposite consists of nitrogen (41.71 wt%), zinc (20.36 wt%) and carbon (33.93 wt%). The comparison of X-ray energy diffraction patterns of the nanocomposite and its components indicates the formation of the nanocomposite.

Figure 10 shows the distribution map of oxygen, carbon, and zinc on the surface of PVA/pectin/ZnO nanocomposite. In addition, the map illustrates the distribution of these elements in the overall composition of the obtained nanocomposite. The results confirmed the formation of the nanocomposite, revealing its final structure and the distribution of its components.

Thermal properties

Figure 11 shows the results of thermogravimetric analysis of PVA, pectin and nanocomposite. Degradation of pure PVA occurred in three stages (Fig. 11a). Evaporation of the remaining moisture in the polymer is responsible for the mass loss at 100°C. At temperatures between 200 and 400°C the polymer loses most of its mass. While the primary chain of PVA decomposes at higher temperatures, the side chains decompose at lower temperatures. Thermal decomposition at temperatures above 400°C is associated with the secondary decomposition of the residues after the primary decomposition stage [34].

In Fig. 11b, we can see the three-stage weight loss process of pure pectin. First, up to 100°C, there is free water diffusion. Then, between 100 and 180°C, there is limited water evaporation. Finally, over 180°C, the polymer chains degrade. At temperatures between 180 and 350°C, pectin showed the greatest weight loss, which is attributable to the breakdown of polymer chains, with values reaching 42%. Destroying glycosidic bonds occurred in this range. The breakdown of the nanocomposite is postponed by the incorporation of ZnO nanoparticles (Fig. 11c). The thermal stability is enhanced by the inclusion of ZnO nanoparticles; however, the peaks of the maximum degradation rate were barely affected. These findings provide more evidence that the highest levels of matrix-filler adhesion and filler dispersion in the polymer matrix were responsible for the most robust interactions among pectin, PVA, and ZnO nanoparticles [35].

CONCLUSIONS

PVA/pectin/ZnO nanocomposites were developed. Taguchi method combined with Qulitek-4 software was used to optimize the composition and processing conditions of nanocomposites. UV-Vis, FT-IR, XRD, SEM, TEM, EDS, MAP and TGA analysis confirmed the formation of PVA/pectin/ZnO nanocomposites with strong antibacterial activity depending on their composition. The developed nanocomposites can be used in dentistry in root canal treatment or as a component of mouthwashes.

Authors contribution

M.S. – research concept, methodology, investigation; R.A. – conceptualization, investigation; M.S.M. – investigation, data analysis; R.S. – supervision, research concept; L.S.W. – resources, writing-review and editing; S.R. – conceptualization, methodology, writing-original draft; A. – visualization, writing-original draft; S.A. supervision, validation, writing-review and editing.

Funding

The research was funded by the Kermanshah University of Medical Sciences under Grant No 4020420.

Conflict of interest

The authors declare that they have no known competing financial interests or personal relationships that could have appeared to influence the work reported in this paper.

REFERENCES

[1] Roberts A.P., Mullany P.: *Expert Review of Anti-infective Therapy* **2010**, *8(12)*, 1441. https://doi.org/10.1586/eri.10.106

[2] Zijnge V., van Leeuwen M.B.M., Degener J.E. *et al.*: *PLoS One* **2010**, *5(2)*, e9321. https://doi.org/10.1371/journal.pone.0009321

[3] Prada I., Micó-Muñoz P., Giner-Lluesma T. *et al.*: *Medicina Oral Patologia Oral y Cirugia Bucal* **2019**, *24(3)*, e364. https://doi.org/10.4317/medoral.22907

[4] Law A., Messer H.: *Journal of Endodontics* **2004**, *30(10)*, 689. https://doi.org/10.1097/01.don.0000129959.20011.ee

[5] Saafan A., Zaazou M.H.: *Open Access Macedonian Journal of Medical Sciences* **2018**, *6*, 1289. https://doi.org/10.3889/oamjms.2018.241

[6] Sharifi R., Vatani A., Sabzi A *et al.*: *Heliyon* **2024**, *10(15)*, e34673. https://doi.org/10.1016/j.heliyon.2024.e34673

[7] Mohammadi H., Moradpoor H., Beddu S. *et al.*: *Heliyon* **2025**, *11(3)*, 42169. https://doi.org/10.1016/j.heliyon.2025.e42169

[8] Safaei M., Moghadam A.: *Materials Today: Communications* **2022**, *31*, 103698. https://doi.org/10.1016/j.mtcomm.2022.103698

[9] Luo L., Huang W., Zhang J. *et al.*: *ACS Applied Nano Materials* **2024**, *7(3)*, 2529. https://doi.org/10.1021/acsanm.3c05615

[10] Jiang W., Mashayekhi H., Xing B.: *Environmental Pollution* **2009**, *157(5)*, 1619. http://doi.org/10.1016/j.envpol.2008.12.025

[11] Safaei M., Salmani M., Azizi B. *et al.*: *Polimery* **2024**, *69(6)*, 362. https://doi.org/10.14314/polimery.2024.6.4

[12] Stoimenov P.K., Klinger R.L., Marchin G.L. *et al.*: *Langmuir* **2002**, *18(17)*, 6679. https://doi.org/10.1021/la0202374

[13] Safaei M., Bahrami M., Wong L.S. *et al.*: *Journal of Applied Organometallic Chemistry* **2025**, *5*, 88. https://doi.org/10.48309/jaoc.2025.471858.1264

[14] Yamamoto O.: *International Journal of Inorganic Materials* **2001**, *3(7)*, 643. https://doi.org/10.1016/S1466-6049(01)00197-0

[15] Jones N., Ray B., Ranjit K.T. *et al.*: *FEMS Microbiology Letters* **2008**, *279(1)*, 71. https://doi.org/10.1111/j.1574-6968.2007.01012.x

[16] Kolodziejczak-Radzimska A., Jesionowski T.: *Materials* **2014**, *7(4)*, 2833. https://doi.org/10.3390/ma7042833

[17] Abebe B., Zereffa E.A., Tadesse A. *et al.*: *Nanoscale Research Letters* **2020**, *15*, 190. https://doi.org/10.1186/s11671-020-03418-6

[18] Raghupathi K.R., Koodali R.T., Manna A.C.: *Langmuir* **2011**, *27(7)*, 4020. https://doi.org/10.1021/la104825u

[19] Muppalaneni S.: *Journal of Developing Drugs* **2013**, *2(3)*, 1. https://doi.org/10.4172/2329-6631.1000112

[20] Takeuchi I., Kato Y., Makino K.: *Journal of Oleo Science* **2021**, *70(3)*, 341. https://doi.org/10.5650/jos.ess20299

[21] Sriamornsak P.: *Expert Opinion on Drug Delivery* **2011**, *8(8)*, 1009. https://doi.org/10.1517/17425247.2011.584867

[22] Liu L.S., Fishman M.L., Hicks K.B.: *Cellulose* **2007**, *14*, 15. https://doi.org/10.1007/s10570-006-9095-7

[23] Al-Gorair A.S., Sayed A., Mahmoud G.A.: *Polymers* **2022**, *14(3)*, 567. https://doi.org/10.3390/polym14030567

[24] Ghorbani F., Gorji P., Mobarakeh M.S. *et al.*: *Journal of Nanomaterials* **2022**, *2022(1)*, 7255181. https://doi.org/10.1155/2022/7255181

[25] Wang N., Ji Y., Zhu Y. *et al.*: *Experimental and Therapeutic Medicine* **2020**, *19(6)*, 3805. https://doi.org/10.3892/etm.2020.8656

[26] Kim Y.H., Priyadarshi R., Kim J.W. *et al.*: *Polymers* **2022**, *14(21)*, 4711. https://doi.org/10.3390/polym14214711

[27] Devi P.G., Velu A.S.: *Journal of Theoretical and Applied Physics* **2016**, *10(3)*, 233. https://doi.org/10.1007/s40094-016-0221-0

[28] Shamsuri N.A., Zaine S.N., Yusof Y.M. *et al.*: *Ionics* **2020**, *26*, 6083. https://doi.org/10.1007/s11581-020-03753-9

[29] Muthukrishnan M., Shanthi C., Selvasekarapandian S. *et al.*: *Ionics* **2019**, *25*, 203. https://doi.org/10.1007/s11581-018-2568-5

[30] Bharathi D., Bhuvaneshwari V.: *Research on Chemical Intermediates* **2019**, *45*, 2065. https://doi.org/10.1007/s11164-018-03717-9

[31] Rashad M.: *Optical Materials* **2020**, *105*, 109857. https://doi.org/10.1016/j.optmat.2020.109857

[32] Saidi N., Azzaoui K., Ramdani M. *et al.*: *Polymers* **2022**, *14(20)*, 4446. https://doi.org/10.3390/polym14204446

[33] Safaei M., Taran M.: *Journal of Polymers and the Environment* **2022**, *30(5)*, 2066.

https://doi.org/10.1007/s10924-021-02329-6

[34] Yang C.M., Chathuranga K., Lee J.S. *et al.*: *Polymer Testing* **2022**, *116*, 107786. https://doi.org/10.1016/j.polymertesting.2022.107786

[35] Nesic A., Meseldzija S., Cabrera-Barjas G. *et al.*: *Foods* **2022**, *11(3)*, 360. https://doi.org/10.3390/foods11030360

Received 5 V 2025.
Accepted 28 V 2025.

Stowarzyszenie Wychowanków
Politechniki Śląskiej w Gliwicach
oraz
Akademia Marynarki Wojennej
im. Bohaterów Westerplatte w Gdyni,
Polskie Towarzystwo Mechaniki Teoretycznej i Stosowanej
zapraszają do udziału w
XIV Konferencji Naukowo-Technicznej
„DIAGNOSTYKA MATERIAŁÓW INŻYNIERSKICH 2026"
10–17 stycznia 2026 r., Malè, Włochy

Patronat Konferencji:
JM Rektor Politechniki Śląskiej – prof. dr hab. inż. Marek PAWEŁCZYK
JM Rektor Akademii Marynarki Wojennej – kontradmirał prof. dr hab. Tomasz SZUBRYCHT
Przewodniczący Komitetu Naukowego: dr hab. inż. Wojciech BŁAŻEJOWSKI, prof. PWr
Honorowy Przewodniczący Komitetu Organizacyjnego: dr hab. inż. Maciej ROJEK
Przewodnicząca Komitetu Organizacyjnego: dr hab. inż. Małgorzata SZYMICZEK, prof. PŚ

Tematyka konferencji:

- Metodyka badań nieniszczących
- Prognozowanie własności układów technicznych
- Diagnostyka polimerów w protetyce, implantologii, sporcie itp.
- Inteligentne materiały polimerowe
- Diagnostyka procesów wytwarzania
- Monitorowanie procesów syntezy i modyfikacji materiałów polimerowych
- Modelowanie układów i symulacja procesów

Wybrane prace rekomendowanych przez Komitet Naukowy (za dodatkową opłatą) zostaną opublikowane w czasopismach: *Journal of Achievements in Materials and Manufacturing Engineering, Archives of Materials Science and Engineering, Polimery, Archives of Acoustics, Advances in Science and Technology Research Journal – ASTRJ, Archives of Foundry Engineering*

Ważne terminy:
Zgłoszenie udziału – 15 października 2025 r.
Nadesłanie streszczeń – 31 października 2025 r.
Dokonanie opłaty – 31 października 2025 r.

Opłata konferencyjna:

Do 15 października 2025 r.:
Opłata za uczestnictwo: 4700 zł – pokój dwuosobowy
Koszt opłaty osoby towarzyszącej: 4600 zł*)

Po 15 października 2025 r.:
Opłata za uczestnictwo: 4900 zł – pokój dwuosobowy
Koszt opłaty osoby towarzyszącej: 4800 zł*)

Opłata obejmuje: zakwaterowanie, wyżywienie, ubezpieczenie, materiały konferencyjne.
Do kosztu opłaty konferencyjnej należy doliczyć koszt przejazdu autokarem z Gliwic-Malè-Gliwice: 590 zł
Koszt imprez towarzyszących: 280 zł

Miejsce konferencji: **Hotel** Sole*****,** Malé, Włochy

Informacje: polymer.diagnostic@gmail.com, tel. 502 533 317

www.diagem.com.pl